SEMARAK ILMU PUBLISHING

CFD Letters

Journal homepage:
https://semarakilmu.com.my/journals/index.php/CFD_Letters/index
ISSN: 2180-1363

A Study on Oscillatory Micropolar Flow Beyond a Contaminated Micropolar Fluid Sphere

Phani Kumar Meduri [1,*], Vijaya Lakshmi Kunche[1]

[1] Department of Mathematics, School of Advanced Sciences, VIT-AP University, Amaravati, Andhra Pradesh, India

ARTICLE INFO

Article history:
Received 12 June 2023
Received in revised form 10 July 2023
Accepted 12 August 2023
Available online 10 December 2023

Keywords:
micropolar fluid; oscillatory flow; drag force; slip condition; stagnant cap.

ABSTRACT

In this paper, the hypothesis of the axisymmetric rectilinear oscillatory flow beyond a micropolar tainted fluid sphere particle in an incompressible non-Newtonian fluid and also the axisymmetric rectilinear oscillatory flow over a viscous tainted fluid sphere particle in an incompressible Newtonian fluid with small amplitude oscillations have been investigated. The velocity field is exhibited in terms of stream functions, and a slip condition is considered on the boundary. The fluid velocities and microrotation components were derived through analytical procedure. The drag force acting on the particle was also computed and verified for special cases. The real drag and imaginary drag values are numerically extracted for varying slip parameter i.e., $2 \leq s \leq 30$, micro polarity i.e., $8 \leq e \leq 32$, and viscosity ratio i.e., $5 \leq \mu \leq 20$ at a fixed parameter values $k = 0.1, \rho = 0.6, \omega = 0.6,\ t = 0.6$. Graphs and tables are used to display the numerical results. It was observed that there was an inverse proportion between slip parameter values, real drag and direct proportion between slip parameter and imaginary drag, for different viscosity ratio and micro polarity values.

1. Introduction

Scientists have done a lot of research on micropolar fluids since they have so many technological and industrial uses. The scientific study of non-Newtonian fluid is used in a variety of economic and even everyday activities, including inkjet printing, covering, and polymer fabrication. We can better comprehend natural phenomena like the flow of the Earth's mantle and hemodynamic by using non-Newtonian fluid dynamics. Because there are many different types of complicated fluids, there is a vast body of literature addressing analytical and numerical solutions for non-Newtonian flows; yet no single governing equation can encompass all the characteristics of all non-Newtonian fluids. Several non-Newtonian fluid systems are available in this scenario, such as the micropolar fluid model presented by Eringen [1, 2]. Local rotational and couple stresses are shown to have an impact via the micropolar fluid model.

* *Corresponding author.*
E-mail address: phanikumarmeduri@gmail.com (Phani Kumar Meduri)

https://doi.org/10.37934/cfdl.16.2.133150

Researchers and professionals in the field of fluid science have been intrigued by the studies on micropolar liquids. The fact that viscous fluids cannot reflect the comprehensive explanation of fluid movement in numerous bio and economy applications necessitates this consideration. The non-symmetric stress tensor is a distinct and odd type of morphology substance for frigid fluids. In terms of natural frame, it shows materials constructed of molecules thrown out at random in the viscous liquid. Polar fluids encourage changes in micro-rotational, micro-inertial, and couple stress in the organism. Polar fluids are, in general, viscous fluid, ionized, and other physiological liquids that contain suspensions of hard or deformable elements. In short, Eringen [1] was the first to mention micropolar fluid theory. Eringen [2] reported in his work about fluid particles that could spin individually from the gyration and migration of the fluid as a whole. The review article by Ariman *et al.,* [3] and monograph of Lukaszewicz [4], reported valuability of the micropolar theory. Satya Deo and Pankaj Shukla [5] calculated the drag generated by a liquid sphere with non-newtonian liquid moving over it with a non-homogeneous micro rotation vector on the boundary by using an analytic method. Jaiswal and Gupta [6] conducted a sustainable analysis of the steady axisymmetric creeping flow of an incompressible non-Newtonian liquid beyond an immersible Reiner-Rivlin liquid sphere and noticed that the cross-viscosity raises the drag on the Reiner-Rivlin sphere in the non-Newtonian liquid. Pankaj Shukla [7] discussed how the laminar flow of a non-Newtonian liquid beyond a sphere enclosed with a slim liquid sheet and obtained the drag force using a non-zero spin boundary condition for the micros-rotation vector. Mishra and Gupta [8] used the no-slip condition to investigate and analyse the continuous axisymmetric uniform flow of an incompressible non-Newtonian fluid over a permeable sphere holding a solid sphere. The above-mentioned literature is related to works on micropolar fluid.

In the nineteenth century, when the proper boundary conditions were initially studied in fluid mechanics, both no-slip and partial-slip boundary conditions were proposed by Neto *et al.,* [9]. Now-a-days there has been an increased interest in using such slip conditions for microfluidic flows which are observed and utilised by Lok *et al.,* [10, 11].

Gomathy *et al.,* [12] focused on the laminar flow of micropolar fluid beyond a fluid sphere along its axis of symmetry, assuming a uniform stream far away from the body. The no-spin and spin boundary conditions were considered, and the drag force was obtained. Selvi [13] analysed the stable axisymmetric laminar flow of a non-Newtonian fluid around a spherical bubble of micropolar liquid shell filled with permeable material. It was observed that the permeable sphere experienced less drag than a non-Newtonian fluid sphere.

The flow around bubbles or droplets in relative motion inside a fluid has been found to be altered by interface pollution. Some of the typical methods include Micropolar fluidized beds, the degassing of polymeric glasses and melts, the use of polymeric solvents in enhanced oil recovery, etc. although it has a broad range of potential applications. To explain the flow around the polluted bubbles, the stagnant-cap model has widely been the preferred choice Cuenot *et al.,* [14-16]. Sadhal and Jonhnson [17] evaluated drag force and polarized between the maximal, the minimal interfacial tensions, and the volume of captivated surfactant by using mixed boundary conditions. Venkata Swamy and Nanda Kishore [18] investigated the flow and drag phenomena of contaminated bubbles in power-law liquids (both shear thinning and shear thickening) and were numerically explored by using ANSYS Fluent. Ramana Murthy and Phani kumar [19] obtained the drag force value analytically for a Stokes liquid flow beyond a tainted liquid sphere by using no-slip condition. Saboni *et al.,* [20] discussed the laminar flow due to the movement of a liquid drop or a bubble in other immiscible fluid and evaluated the drag force by using mixed boundary conditions. The mentioned investigations here are related to fluid drop and contaminated fluid drop with no-slip condition.

The oscillating flows are produced by inserting bodies that oscillate at a deliberated frequency and amplitude which are used in a variety of ways. The oscillatory flow of microscopic particles in a viscous fluid appears in a wide range of engineering applications such as micro-organism swimming and Brownian particle motion, ultra-filtration, biomechanics of blood flow and other biological or chemical phenomena from Hocquart *et al.,* [21, 22].

Lakshmana Rao and Bhujanga Rao [23] analysed both rectilinear and rotatory oscillations of a sphere along a diameter and illustrated the drag and couple on the rectilinear and rotary oscillating sphere respectively. Srinivasacharya and Iyengar [24] have considered a stationary axisymmetric body that is placed in an incompressible micropolar fluid by the flow of more rectilinear oscillations along its axis of symmetry and drag force is obtained using an analytic method. They reduced the special cases of spheroid and sphere. Naveed *et al.,* [25] briefly examined how heat is transmitted when a micropolar fluid flows over an oscillating, curved flexible surface in a time-dependent hydromagnetic way, using the enhanced version of the heat flow model, conduction of convection. These are a few works related to oscillatory flow.

Mishra *et al.,* [27] considered the free convective micropolar fluid across a shrinking sheet in the existence of a heat source/sink with Runge-Kutta method and the shooting methodology. The effects of pertinent variables that characterised the flow graphically displayed. Ilyas *et al.,* [26] explored to enhance the water barrier qualities of the sugar palm starch (SPS)-based films, sugar palm nano fibrillated cellulose (SPNFCs) nanocomposites were cast and used as biodegradable reinforcement materials and observed the compatibility among SPNFCs and SPS matrices, which was confirmed through FESEM. Ali Bagh *et al.,* [28] investigated the importance of suction/injection for gravity modifying mixed convection in micropolar fluid flow caused by an inclined sheet in the presence of magnetic field and radiation of heat. This research is unique in that it considers how g-jitter affects the dynamics of a micropolar fluid with adjustable sheet tilt. Siddiqa *et al.,* [29] examined the behaviour of conjugate natural convection across a finite vertical surface submerged in a micropolar fluid during strong thermal radiation through the implicit finite difference Keller-box method. For different values of the micropolar or material parameter, K, the conjugate parameter, B, and the thermal radiation parameter, Rd, the characteristics of fluid flow and heat transmission are analysed and visually displayed. Jamali *et al.,* [30] used the finite element approach to analyse the generalised power law theory of blood flow in a bifurcated artery that has undergone various degrees of blockage. Al-Dailami, Anas *et al.,* [31] studied various PBR kinds and their characteristics before elaborating on PBRs' potential for microalgae development. Kumar Manoj, and Aadil Hashim Saifi [32] focused on a water capillary bridge that is enclosed in silicone oil and is bordered by two solid insulated discs. In terms of the highest interfacial velocities, net heat transmitted to the bridge, and locations of the stagnation points, we notice major variations among heater and cooler setups.

Applications of micropolar fluid, slip, oscillating flow are mentioned above. The extensive studies by eminent authors on micropolar fluid sphere, contaminated fluid sphere and oscillating flow etc. are presented.

However, no hypothesis of the flow generated by the rectilinear oscillation over a Newtonian and non-Newtonian contaminated fluid sphere using slip conditions have been reported. This inspired us to explore the most current problem. We have considered problems of oscillatory flow of micropolar fluid beyond a partially contaminated micropolar fluid sphere, viscous contaminated fluid sphere particle in a Newtonian fluid using slip beyond the barrier, Shear stress that continues to apply to the clean area, and regularity state far from the body in the present work. The velocity components that are obtained and are described in terms of the stream function, exact solution, and drag force are under examination.

This paper is organised with formulation of the problem, study on oscillatory flow of micropolar beyond a micropolar contaminated fluid sphere, followed by oscillatory viscous fluid past a viscous contaminated fluid sphere, results and discussion and conclusions.

2. Modelling

2.1 Basic Equations

We know momentum equation from Eringen [1, 2] as

$$\frac{\partial \rho}{\partial t} + div(\rho V) = 0, \tag{1}$$

$$\rho \frac{dV}{dt} = \rho f - \nabla p + k\nabla \times w - (\mu + k)\nabla \times \nabla \times V + (\lambda + 2\mu + k)\nabla(div\, V), \tag{2}$$

$$\rho J \frac{dw}{dt} = \rho I - 2kw + k\nabla \times V - \gamma \nabla \times \nabla \times w + (\alpha + \beta + \gamma)\nabla(div\, w). \tag{3}$$

where f body forces per unit mass, I microrotation factors per unit mass, J the gyration factor, V the velocity field, w the microrotation field, and p the pressure, the α, β, γ are gyroviscosity factors that correspond to the following inequalities and μ the classical viscosity coefficients k, λ, μ vortex viscosity factors.

$$3\alpha + \beta + \gamma \geq 0,\ 2\mu + k \geq 0,\ 3\lambda + 2\mu + k \geq 0 \quad , \gamma \geq |\beta|, k \geq 0, \gamma \geq 0. \tag{4}$$

2.2 Oscillatory Flow of Micropolar Beyond a Micropolar Contaminated Fluid Sphere

Consider a fluid sphere which is fixed in an oscillatory fluid flow (see Figure 1). The flow is assumed to be axisymmetric and incompressible. The contaminations in the fluid are accumulated to the rear end of the fluid sphere to form a cap region. Let $x_0 = \cos\theta$ be the varying point on the surface. The cap region is from $x_0 < x < 1$ and the free surface (no-cap region) is from $-1 < x < x_0$. If x_0 tends to -1 then the surface of the fluid sphere is covered by a cap and becomes as a solid sphere. Also, when x_0 tends to 1, then the surface acts as a fluid sphere. Here in the manuscript we assumed the surface is partially covered with a cap region.

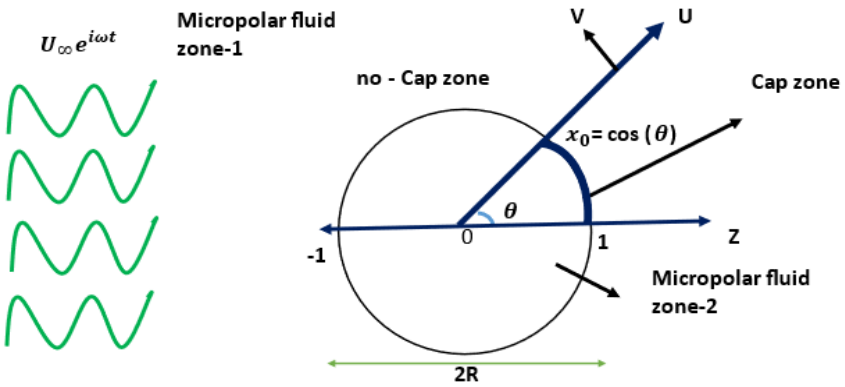

Fig. 1. Geometry of oscillatory flow of non-Newtonian liquid past a fluid sphere

Let $(R, \theta, \emptyset)$ represents for spherical polar coordinates, with the origin at the center of a sphere with radius a, scale factors of $h_1 = 1$, $h_2 = R$ and $h_3 = Rsin\theta$ and basis unit vectors of, $(\bar{e}_r, \bar{e}_\theta, \bar{e}_\emptyset)$, with Z-axis parallel to the flow direction.

The velocity and angular rotation of the flow field as

$$U = (u_{r,} u_\theta, 0) \ , \qquad V = (0,0, v_\emptyset) \ .$$

In the view of the axisymmetric flow, the velocity elements represented in measures of stream function Ψ as

$$u_r = \frac{1}{R^2 sin\theta} \frac{\partial \Psi}{\partial \theta} \ , \ u_\theta = -\frac{1}{Rsin\theta} \frac{\partial \Psi}{\partial r}.$$

Assume the flow is oscillatory with a velocity $U_\infty e^{i\omega t}\, \overline{k}$ along the axis of symmetry $\theta = 0$ in an infinite region with small amplitude. Here, ω is the oscillation frequency, and all flow variables are independent of $\emptyset$. The velocity and microrotation factors are selected as

$$V = \left(\nabla \times \frac{\Psi\, \overline{e_\phi}}{h_3}\right) e^{i\omega t} = \left(\frac{1}{R^2 sin\theta} \frac{\partial \Psi}{\partial \theta} \overline{e_r} - \frac{1}{Rsin\theta} \frac{\partial \Psi}{\partial R} \overline{e_\theta}\right) e^{i\omega t} \tag{5}$$

$$\nabla \times V = -\left(\frac{E_0^2 \Psi}{h_3}\right) \overline{e_\theta} e^{i\omega t}; \nabla \times \nabla \times \nabla \times V = -\left(\frac{E_0^4 \Psi}{h_3}\right) \overline{e_\theta} e^{i\omega t};$$

$$w = \frac{C}{Rsin\theta} e^{i\omega t}\, \overline{e_\phi} \ . \tag{6}$$

Substituting the above expressions (5), (6) in (2), (3) we have

$$\rho i\omega V = -\nabla P + k\nabla \times w - (\mu + k)\, \nabla \times \nabla \times V, \tag{7}$$

$$i\rho j\omega w = -2\mathrm{k}w + k\nabla \times V - \gamma\, \nabla \times \nabla \times w. \tag{8}$$

The pressure terms are obtained as

$$\frac{\partial P}{\partial R} = -\frac{i\sigma U_\infty (\mu + k)}{a} \frac{1}{R^2 sin\theta} \frac{\partial \Psi}{\partial \theta},$$

$$\frac{\partial P}{\partial \theta} = \frac{i\sigma U_\infty (\mu + k)}{a} \frac{1}{sin\theta} \frac{\partial \Psi}{\partial R}.$$

Eliminating pressure and applying curl for (7) we get

$$(\mu + k)\, E_0^4\, \Psi + kE_0^2 C = i\rho\omega E_0^2 \Psi, \tag{9}$$

where $E_0^2 = \frac{\partial^2}{\partial R^2} + \frac{1}{R^2} \frac{\partial^2}{\partial \theta^2} - \frac{cot\theta}{R^2} \frac{\partial}{\partial \theta}$. (10)

Applying curl of curl to Eq. (8) we get

$$kE_0^4\Psi = -(2k + i\rho j\omega)(E_0^2\, C) + \gamma\,(E_0^4\, C). \tag{11}$$

Substituting $E_0^2 C$ from Eq. (9) in Eq. (11) we get

$$E_0^2\left(E_0^2 - \frac{\delta_1^2}{a^2}\right)\left(E_0^2 - \frac{\delta_2^2}{a^2}\right)\Psi = 0. \tag{12}$$

$$\left.\begin{aligned}\delta_1^2 + \delta_2^2 &= \frac{\{k(2\mu+k)+i\rho\omega(j\mu+jk+\gamma)\}a^2}{\gamma(\mu+k)},\\ \delta_1^2\delta_2^2 &= \frac{i\rho\omega(2k+ji\rho\omega\gamma)a^4}{\gamma(\mu+k)}.\end{aligned}\right\} \tag{13}$$

From Eq. (8)

$$(2k + \rho i\omega j)C = \gamma E_0^2 C - k\, E_0^2\Psi. \tag{14}$$

Substituting Eq. (9) in Eq. (14) we get

$$(2k + \rho i\omega j)C = \frac{1}{k}E_0^2\big((\gamma i\rho\omega - k^2)\Psi - (\mu + k)\gamma E_0^2\Psi\big). \tag{15}$$

Using non-dimensional scheme

$R = ra, E_0^2 = \frac{E^2}{a^2},\ \Psi = \psi U_\infty a^2,\ C = \boldsymbol{C}U_\infty,\ c = \frac{k}{(\mu+k)},\ \sigma = \rho\omega a^2(\mu + k),\ J = \rho\omega j a^2/\gamma$. Eq. (12)

changes as

$$E^2(E^2 - \delta_1^2)\,(E^2 - \delta_2^2)\psi = 0, \tag{16}$$

$$c\boldsymbol{C} = -\frac{i\sigma}{\delta_1^2\delta_2^2}E^2\big(E^2 - (\delta_1^2 + \delta_2^2)\big)\psi - E^2\psi. \tag{17}$$

In view of the linearity and commutativity of the operators $E^2, (E^2 - \delta_1^2) and (E^2 - \delta_2^2)$ the solution of (16) can be obtained by the superposition. The solutions of

$$E^2\psi_0 = 0, \tag{18}$$

$$(E^2 - \delta_1^2)\psi_1 = 0, \tag{19}$$

$$(E^2 - \delta_2^2)\psi_2 = 0, \tag{20}$$

expressing the solution in the form $\psi = \psi_0 + \psi_1 + \psi_2$.

To match uniform velocity at infinity, the solution for ψ can be assumed in the form,

$$\psi_e(r,x) = \begin{cases}\psi_{en}(r)G_2(x) & for\ \ -1 < x < x_0\ (no - cap\ region)\\ \psi_{ec}(r)G_2(x) & for\ \ x_0 < x < 1\ \ (cap\ region\ )\end{cases} \tag{21a}$$

$$\psi_i(r,x) = \begin{cases} \psi_{in}(r)G_2(x) & for \ \ -1 < x < x_0 \ (no-cap \ region) \\ \psi_{ic}(r)G_2(x) & for \ \ x_0 < x < 1 \ \ (cap \ region) \end{cases} \quad (21b)$$

Here ψ_{en}, ψ_{ec} are external stream function for no-cap, cap regions. Also, ψ_{in}, ψ_{ic} represent inner tream function with no-cap and cap zones respectively and the microrotation components $\boldsymbol{C}_{en}, \boldsymbol{C}_{ec}, \boldsymbol{C}_{in}, \boldsymbol{C}_{ic}$ satisfies the Eq. (11) and Eq. (15) and these are to be solved using appropriate conditions on the boundary and regularity condition at infinity

By separation of variables method, external stream functions are obtained as

$$\psi_{en} = \left(r^2 + \frac{f_1}{r} + g_1\sqrt{r}K_{\frac{3}{2}}(\delta_{1en}r) + h_1\sqrt{r}K_{\frac{3}{2}}(\delta_{2en}r)\right)G_2(x), \quad (22)$$

$$\psi_{ec} = \left(r^2 + \frac{f_2}{r} + g_2\sqrt{r}K_{\frac{3}{2}}(\delta_{1ec}r) + h_2\sqrt{r}K_{\frac{3}{2}}(\delta_{2ec}r)\right)G_2(x). \quad (23)$$

Internal stream functions are

$$\psi_{in} = (f_3r^2 + g_3\sqrt{r}I_{\frac{3}{2}}(\delta_{1in}r) + h_3\sqrt{r}I_{\frac{3}{2}}(\delta_{2in}r))G_2(x), \quad (24)$$

$$\psi_{ic} = (f_4r^2 + g_4\sqrt{r}I_{\frac{3}{2}}(\delta_{1ic}r) + h_4\sqrt{r}I_{\frac{3}{2}}(\delta_{2ic}r))G_2(x). \quad (25)$$

For no-cap region $f_4 = g_4 = h_4 = 0$, thus, $\Rightarrow \psi_{ic} = 0$,

where $I_{\frac{3}{2}}$, $K_{\frac{3}{2}}$ are Modified Bessel's function and $G_2(x)$ is a Gegenbauer functions (M. Abramowitz and I.A. Stegun [27])

The parameters $f_1, g_1, h_1, f_2, g_2, h_2, f_3, g_3, h_3$ in (22) - (24) are calculated by the following boundary conditions:

2.2.1 Boundary conditions

(i) Regularity conditions far away from the body

$$\lim_{r\to\infty} \psi_e = \frac{1}{2}Ur^2sin^2\theta \ \text{(Zone – 1) and}$$
$$\lim_{r\to 0} \psi_i = \ \text{finite (Zone – 2).} \quad (26)$$

(ii) Normal velocity is zero on the boundary

$$\psi_{en} = \psi_{ec} = \psi_{in} = \psi_{ic} = 0 \qquad \text{on} \ \ r = 1. \quad (27)$$

(iii) Slip condition: Tangential velocity is proportional to the tangential stress along the surface (Happel and Brenner [26])

$$\tau_{r\theta} = \beta(v_{\theta e} - v_{\theta i}) \quad \text{on} \ \ r = 1, \quad \text{where } \beta \text{ is a sliding friction coefficient.} \quad (28)$$

(iv) Tangential Stress is continuous across the surface i.e.,

$$\tau_{r\theta e} = \tau_{r\theta i} \qquad \text{on} \quad r = 1. \tag{29}$$

(v) The angular velocity zero on the boundary

i.e., $C\ is\ 0$ on $r = 1 \Rightarrow C_{en} = C_{ec} = C_{in} = C_{ic} = 0$. (30)

Microrotation Components C in Eq. (17) for external and internal flow reduces to

$$cC_{en} = \sqrt{r}\left\{g_1(i\sigma - \delta_{1en}^2)K_{\frac{3}{2}}(\delta_{1en}r) + h_1(i\sigma - \delta_{2en}^2)K_{\frac{3}{2}}(\delta_{2en}r)\right\}G_2(x), \tag{31}$$

$$cC_{ec} = \sqrt{r}\left\{g_2(i\sigma - \delta_{1ec}^2)K_{\frac{3}{2}}(\delta_{1ec}r) + h_2(i\sigma - \delta_{2ec}^2)K_{\frac{3}{2}}(\delta_{2ec}r)\right\}G_2(x), \tag{32}$$

$$cC_{in} = \sqrt{r}\left\{g_3(i\sigma - \delta_{1in}^2)I_{\frac{3}{2}}(\delta_{1in}r) + h_3(i\sigma - \delta_{2in}^2)I_{\frac{3}{2}}(\delta_{2in}r)\right\}G_2(x), \tag{33}$$

$$cC_{ic} = \sqrt{r}\left\{g_4(i\sigma - \delta_{1ic}^2)I_{\frac{3}{2}}(\delta_{1ic}r) + h_4(i\sigma - \delta_{2ic}^2)I_{\frac{3}{2}}(\delta_{2ic}r)\right\}G_2(x). \tag{34a}$$

2.2.2 Solution

Using the boundary condition Eq. (26) - (30), we get nine equations with nine unknowns as

$$f_1 + g_1' + h_1' = -1, f_2 + g_2' + h_2' = -1, f_3 + g_3' + h_3' = 0,$$

$$-6f_1 - g_1'\left(z_{2n}\delta_{1en}^2 + 4 + 2\Delta_1(\delta_{1en})\right) - h_1'\left(z_{2n}\delta_{2en}^2 + 4 + 2\Delta_1(\delta_{2en})\right) + g_3'\left(\delta_{1in}^2 z + 4 + 2\Delta_3(\delta_{1in})\right) + h_3'\left(\delta_{2in}^2 z + 4 + 2\Delta_3(\delta_{2in})\right) = 0,$$

$$f_1(-6 - sz_{1n}) + g_1'\left(-z_{2n}\delta_{1en}^2 - 4 - 2\Delta_1(\delta_{1en}) - sz_1\Delta_1(\delta_{1en})\right) + h_1'\left(-z_{2n}\delta_{2en}^2 - 4 - 2\Delta_1(\delta_{2en}) - sz_{1n}\Delta_1(\delta_{2en})\right) + g_3' sz_{1n}\Delta_3(\delta_{1in}) - 2f_3 sz_{1n} + h_3'\Delta_3(\delta_{2in})sz_{1n} = (-2z_{1n})s,$$

$$f_2(-6 - sz_{1c}) + g_2'\left(-z_{2c}\delta_{1ec}^2 - 4 - 2\Delta_1(\delta_{1ec}) - sz_1\Delta_1(\delta_{1ec})\right) + h_2'\left(-z_{2c}\delta_{2ec}^2 - 4 - 2\Delta_1(\delta_{2ec}) - sz_{1c}\Delta_1(\delta_{2ec})\right) = (-2z_{1c})s,$$

$$g_1'(\mathrm{i}\sigma - \delta_{1\mathrm{en}}^2) + h_1'(\mathrm{i}\sigma - \delta_{2\mathrm{en}}^2) = 0, g_2'(\mathrm{i}\sigma - \delta_{1\mathrm{ec}}^2) + h_2'(\mathrm{i}\sigma - \delta_{2\mathrm{ec}}^2) = 0,$$

$$g_3'(\mathrm{i}\sigma - \delta_{1\mathrm{in}}^2) + h_3'(\mathrm{i}\sigma - \delta_{2\mathrm{in}}^2) = 0,$$

and $f_4 = g_4' = h_4' = 0,$

Where,

$$g_1' = g_1K_{\frac{3}{2}}(\delta_{1en}), g_2' = g_2K_{\frac{3}{2}}(\delta_{1ec}), g_3' = g_3I_{\frac{3}{2}}(\delta_{1in}), h_1' = h_1K_{\frac{3}{2}}(\delta_{2en}), h_2' = h_2K_{\frac{3}{2}}(\delta_{2ec}),$$

$h_3' = h_3 I_{\frac{3}{2}}(\delta_{2in})$, slip parameter$(s) = \frac{\beta a}{\mu}$, $\Delta_1(\delta_{1en}) = 1 + \frac{\delta_{1en} K_{\frac{1}{2}}(\delta_{1en})}{K_{\frac{3}{2}}(\delta_{1en})}$, $\Delta_1(\delta_{1ec}) = 1 + \frac{\delta_{1ec} K_{\frac{1}{2}}(\delta_{1ec})}{K_{\frac{3}{2}}(\delta_{1ec})}$, $\Delta_2(\delta_{1in}) = 1 + \frac{\delta_{1in} I_{\frac{1}{2}}(\delta_{1in})}{I_{\frac{3}{2}}(\delta_{1in})}$, $\Delta_2(\delta_{2ic}) = 1 + \frac{\delta_{2ic} I_{\frac{1}{2}}(\delta_{2ic})}{I_{\frac{3}{2}}(\delta_{2ic})}$, $\Delta_3(\delta_{1in}) = 1 + \frac{\delta_{1in} I_{\frac{1}{2}}(\delta_{1in})}{I_{\frac{3}{2}}(\delta_{1in})}$,

$z_{1n} = \frac{2(1-C_{en})}{2-C_{en}}$, $z_{2n} = \frac{2}{2-C_{en}}$, $z_{2c} = \frac{2}{2-C_{ec}}$, $z_{1c} = \frac{2(1-C_{ec})}{2-C_{ec}}$.

Cross viscosity parameter $c_{en} = \frac{k_{en}}{\mu_{en}+k_{en}}$, $c_{ec} = \frac{k_{ec}}{\mu_{ec}+k_{ec}}$, $c_{in} = \frac{k_{in}}{\mu_{in}+k_{in}}$, $c_{ic} = \frac{k_{ic}}{\mu_{ic}+k_{ic}}$.

Solving the above system of equations analytically, we get the values of parameters as

$$\left.\begin{array}{l} f_1 = -1 + h_1'(\epsilon_{en} - 1)\,, f_2 = -1 + h_2'(\epsilon_{ec} - 1)\;\; f_3 = -h_3'(\epsilon_{in} - 1), \\ g_1' = -h_1'\epsilon_{en}\,,\;\; g_2' = -h_2'\epsilon_{ec}\;\,, g_3' = -h_3'\epsilon_{in}, \\ h_1' = \frac{(-3z_{1n}s-6)L_2'+6L_2}{\eta_1}, h_2' = \frac{(-3z_{1c}s-6)}{L_3},\;\; h_3' = \frac{-6L_1+(3sz_{1n}+6)L_1'}{\eta_1}. \end{array}\right\} \quad (34b)$$

Here $\eta_1 = L_1 L_2' - L_2 L_1'$,

Here,

$L_1 = 2(1-\epsilon_{en}) + z_{2n}(\delta_{1en}^2\epsilon_{en} - \delta_{2en}^2) + 2\Delta_4 + sz_{1n}(1 - \epsilon_{en} + \Delta_4)$,

$L_1' = 2(1-\epsilon_{en}) + z_{2n}(\delta_{1en}^2\epsilon_{en} - \delta_{2en}^2) + 2\Delta_4$,

$L_2 = -sz_{1n}(2(1-\epsilon_{in}) + \Delta_5)$,

$L_2' = 4(1-\epsilon_{in}) - z_n(\delta_{1in}^2\epsilon_{in} - \delta_{2in}^2) - 2(\Delta_5)$,

$L_3 = 2(1-\epsilon_{ec}) + s\, z_{1c}(1 - \epsilon_{ec} + \Delta_6)$,

$\epsilon_{en} = \frac{(\mathrm{i}\sigma-\delta_{2\mathrm{en}}^2)}{(\mathrm{i}\sigma-\delta_{1\mathrm{en}}^2)}$, $\epsilon_{ec} = \frac{(\mathrm{i}\sigma-\delta_{2\mathrm{ec}}^2)}{(\mathrm{i}\sigma-\delta_{1\mathrm{ec}}^2)}$, $\epsilon_{in} = \frac{(\mathrm{i}\sigma-\delta_{2\mathrm{in}}^2)}{(\mathrm{i}\sigma-\delta_{1\mathrm{in}}^2)}$, $\epsilon_{ic} = \frac{(\mathrm{i}\sigma-\delta_{2\mathrm{ic}}^2)}{(\mathrm{i}\sigma-\delta_{1\mathrm{ic}}^2)}$,

$\Delta_4 = (\Delta_1(\delta_{1en})\epsilon_{en} - \Delta_1(\delta_{2en}))$, $\Delta_5 = (\Delta_3(\delta_{1in})\epsilon_{in} - \Delta_3(\delta_{2in}))$, $\Delta_6 = (\Delta_2(\delta_{1ec})\epsilon_{ec} - \Delta_2(\delta_{2ec}))$,

$z_n = \frac{(2-C_{in})^2 k_0 + C_{in}C_0(2-C_{en})}{(2-C_{en})C_o(2-C_{in})}$.

The stream functions values Eq. (22) - (25) and micro rotation component values (31) - (34) of external, internal with cap and no-cap zones were obtained.

2.2.3 Valuate the drag force

The drag force F_z of oscillatory flow of the micropolar fluid is.

$$F_z = i\rho\omega UV_0 + 4\pi i\rho\omega \lim_{r\to\infty} \frac{r(\psi_e - \psi_\infty)}{sin^2\theta}, \qquad \text{(Srinivasa Charya and Iyengar [24])} \tag{35}$$

$$= i\rho\omega UV_0 + 2\pi i\rho\omega \lim_{r\to\infty} \left(f_1 + g_1 r^{\frac{3}{2}} K_{\frac{3}{2}}(\delta_{1en} r) + h_1 r^{\frac{3}{2}} K_{\frac{3}{2}}(\delta_{2en} r) + f_2 + g_2 r^{\frac{3}{2}} K_{\frac{3}{2}}(\delta_{1ec} r) + h_2 r^{\frac{3}{2}} K_{\frac{3}{2}}(\delta_{2ec} r) \right).$$

As $r \to \infty$, $g_1 = h_1 = g_2 = h_2 = 0$ (based on regularity condition),

V_0 = volume of the body $= \frac{4}{3}\pi r^3$.

$$F_z = 2\pi i\rho\omega U_\infty a^3 (f_1 + f_2) e^{i\omega t}. \tag{36}$$

this can be expressed in the form as

$$F_z = M\omega U_\infty (-T' - iT) l_1 e^{i\omega t}. \tag{37}$$

Where M = $2\pi\rho\omega a^3(f_1 + f_2)$, Real drag = $2\pi\rho\omega U_\infty a^3(f_1 + f_2)\sin(\omega t)$,

Imaginary drag = $-2\pi\rho\omega U_\infty a^3(f_1 + f_2)\cos(\omega t)$, $\omega = \frac{\sigma(\mu+k)}{\rho\, a^2}$,

where M is the mass of the fluid laid-out by the sphere.

The drag parameters T and T' are calculated for distinct values of cross viscosity parameter c, frequency parameter σ, and microrotation parameter s.

As $\delta_2 \to \infty$, $\mu \to \infty, s \to \infty$ then it changes to oscillatory viscous flow on the solid sphere by no-slip, which matches to the drag force evaluated by Lakshmana Rao and Bhujanga Rao [23].

2.3 Oscillatory Flow of Viscous Fluid Flow Past a Contaminated Viscous Fluid Sphere

Figure 2 shows the geometry of the problem oscillatory viscous fluid past a viscous contaminated liquid sphere

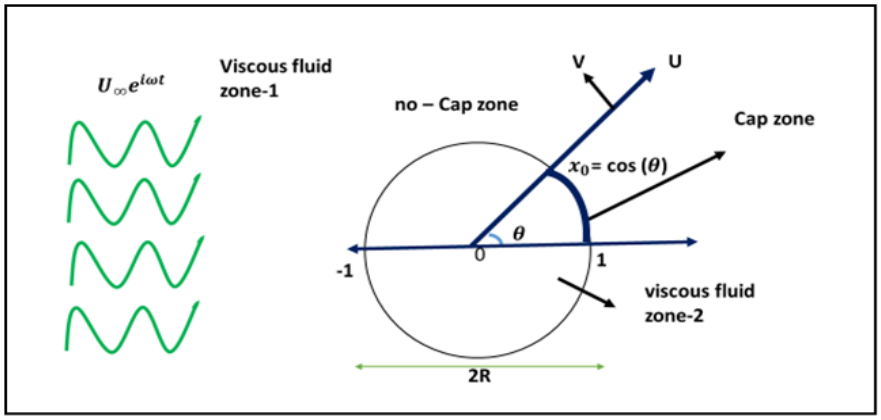

Fig. 2. The geometry of the problem oscillatory viscous fluid past a viscous contaminated liquid sphere

The physical situation and assumptions are same as mentioned below Figure 1. The momentum equation of oscillatory viscous fluid is obtained when $\kappa \longrightarrow 0$ in (7) as

$$E^2(E^2 - \delta_1^2)\,\psi = 0\,, \qquad \text{Where,} \quad \delta_1^2 = \frac{\rho i\omega}{\mu} \tag{38}$$

The external and internal stream functions satisfying (38) are given by ψ_e, ψ_i respectively.

By separation of variables method, we get external functions as

$$\psi'_{en} = \left(r^2 + \frac{f_1}{r} + g_1\sqrt{r}K_{\frac{3}{2}}(\delta_{1en}r)\right)G_2(x), \tag{39}$$

$$\psi'_{ec} = \left(r^2 + \frac{f_2}{r} + g_2\sqrt{r}K_{\frac{3}{2}}(\delta_{1ec}r)\right)G_2(x). \tag{40}$$

And internal stream functions are obtained as

$$\psi'_{in} = (f_3 r^2 + g_3\sqrt{r}I_{\frac{3}{2}}(\delta_{1in}r))G_2(x), \tag{41}$$

$$\psi'_{ic} = (f_4 r^2 + g_4\sqrt{r}I_{\frac{3}{2}}(\delta_{1ic}r))G_2(x). \tag{42}$$

For cap region, $\psi'_{ic} = 0$.

The arbitrary constants in (39) - (41) are calculated by using boundary conditions.

2.3.1 Boundary conditions

(i) Regularity conditions:

$$\lim_{r\to\infty}\psi_e = \frac{1}{2}Ur^2\sin^2\theta \text{ (Zone – 1) and}$$
$$\lim_{r\to 0}\psi_i = \text{ finite (Zone – 2)} \tag{43}$$

(ii) Normal velocity is zero on the boundary condition

$$\psi'_{en} = \psi'_{ec} = \psi'_{in} = \psi'_{ic} = 0 \qquad \text{on} \quad r = 1. \tag{44}$$

(iii) Slip condition: Tangential velocity is proportional to the tangential stress along the surface (Happel and Brenner [26])

$$\tau_{r\theta e} = \beta(v_{\theta e} - v_{\theta i}) \quad \text{on} \quad r = 1\,. \tag{45}$$

(iv) Tangential Stress is continuous across the surface i.e.,

$$\tau_{r\theta e} = \tau_{r\theta i} \qquad \text{on} \quad r = 1. \tag{46}$$

2.3.2 Solution

Using the boundary condition (43) - (46), we get six equations with six unknowns as

$$\left.\begin{aligned} &f_1 + g_1' = -1,\ f_2 + g_2' = -1, f_3 + g_3' = 0, \\ &f_1(4+s) + 2f_3 s + g_1'(\delta_{1en}^2 + 2 + \Delta_1(\delta_{1en})(s+2)) - s g_3' \Delta_2(\delta_{1in}) = 2s + 2, \\ &f_2(4+s) + g_2'(\delta_{1ec}^2 + 2 + \Delta_1(\delta_{1ec})(s+2)) = 2s + 2, \\ &4f_1 + g_1'\left(\delta_{1en}^2 + 2 + 2\Delta_1(\delta_{1en})\right) - \mu\left(-2f_3 + g_2'\left(\delta_{1in}^2 + 2 + 2\Delta_2(\delta_{1in})\right)\right) = 2, \end{aligned}\right\} \quad (47)$$

and $f_4 = g_4' = 0$.

Solving the above system of equations analytically, we get the values of parameters as

$$\left.\begin{aligned} &f_1 = -1 - g_1',\ f_2 = -1 - g_2',\ \ f_3 = -g_3', \\ &g_1' = \frac{(3s+6)A_4 - 6A_2}{A_5},\ g_2' = \frac{(3s+6)}{(s+2)(\Delta_1(\delta_{1ec}) - 1) + \delta_{1ec}^2},\ \ g_3' = \frac{6A_1 - (3s+6)A_3}{A_5}, \end{aligned}\right\} \quad (48)$$

here $A_5 = A_3 A_2 - A_1 A_4$,

Where,

$$A_1 = (s+2)(\Delta_1(\delta_{1en}) - 1) + \delta_{1en}^2, \quad A_2 = s\left(-2 - \Delta_2(\delta_{1in})\right),$$

$$A_3 = -2 + 2\Delta_1(\delta_{1en}) + \delta_{1en}^2\ ,\ A_4 = -\mu\left(\delta_{1in}^2 + 4 + 2\Delta_2(\delta_{1in})\right).$$

Thus, the stream functions values (39) - (42) are obtained.

2.3.3 Evaluate the drag force

The drag force F_z experienced by body with oscillatory flow in limiting form as given by Srinivasa Charya and Iyengar [24] is

$$\begin{aligned} F_z &= i\rho\omega U V_0 + 4\pi i\rho\omega \lim_{r\to\infty} \frac{r(\psi_e - \psi_\infty)}{sin^2\theta} \\ &= i\rho\omega U V_0 + 2\pi i\rho\omega \lim_{r\to\infty} \left(f_1 + g_1 r^{\frac{3}{2}} K_{\frac{3}{2}}(\delta_{1en} r) + f_2 + g_2 r^{\frac{3}{2}} K_{\frac{3}{2}}(\delta_{1ec} r)\right) \end{aligned} \quad (49)$$

As $r \to \infty$, $g_1 = g_2 = 0$ (based on regularity condition), V_0 = volume of the body $= \frac{4}{3}\pi r^3$.

The expression for the drag then becomes.

$$F_z = 2\pi i\rho\omega U_\infty a^3 (f_1 + f_2) e^{i\omega t}. \quad (50)$$

Eq. (50) can be expressed in the form.

$$F_z = M\omega U_\infty(-T1 - iT)l_1 e^{i\omega t}, \tag{51}$$

where M = $2\pi\rho\omega a^3(f_1 + f_2)$, Real drag = $2\pi\rho\omega U_\infty a^3(f_1 + f_2)\sin(\omega t)$,

Imaginary drag = $-2\pi\rho\omega U_\infty a^3(f_1 + f_2)\cos(\omega t)$, $\omega = \frac{\sigma(\mu+k)}{\rho\, a^2}$, where M is the mass of the fluid laid-out by the sphere.

The drag parameters T and $T1$ are evaluated for various values of frequency parameter σ, and slip parameter s. As $\mu \to \infty, s \to \infty$, we get the case of the solid sphere by no-slip, which matches to the drag force calculated by Lakshmana Rao and Bhujanga Rao [23].

3. Results

For an oscillatory flow of micropolar beyond a micropolar contaminated fluid sphere, the real $(T)$and imaginary part $(T1)$ of drag force variations for slip parameters (s) with varying micro polarity e (ϵ values with cap and no-cap zones) i.e., $\epsilon = \frac{(i\sigma - \delta_2^2)}{(i\sigma - \delta_1^2)}$ at fixed values to frequency parameters $\mu = 10, k = 0.1, \rho = 0.6, \omega = 0.6,\ t = 0.6$ are presented numerically and are shown in Figure 3 and Figure 4. Real drag (T) vs Slip parameter (s) at different micro polarity (e) values are plotted in Figure 3. It was noticed that with a rise in slip (s) values there is a fall in real drag (T) and also with an increase in micro polarity (e) values there is a fall in the values of real drag (T). The numerical results are in Table 1 presented.

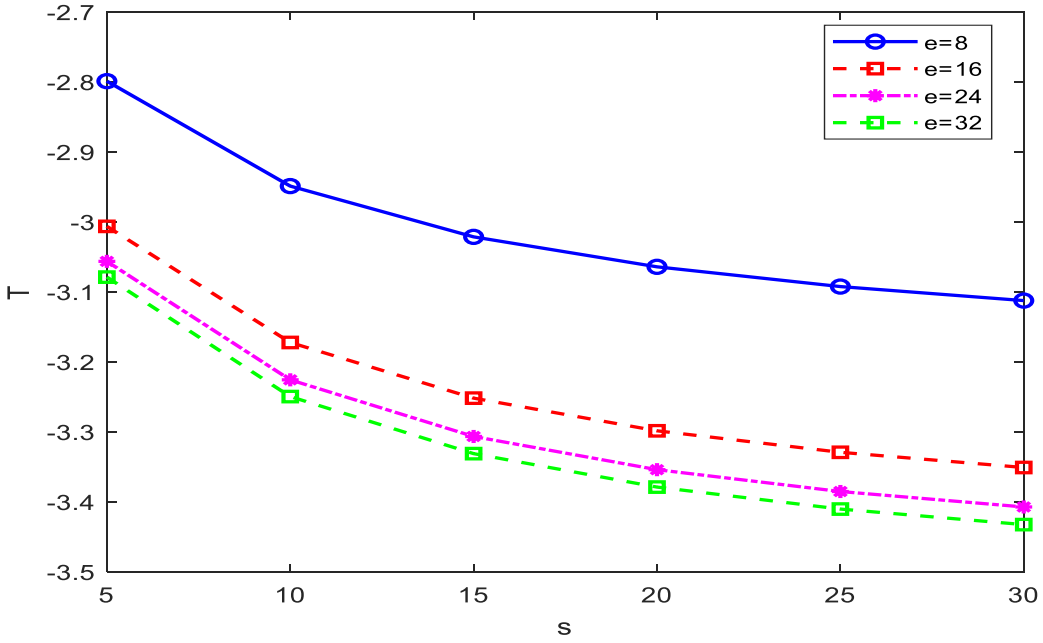

Fig. 3. Real drag(T) vs slip parameter (s) at change of micropolarity (e) values at fixed values to frequency parameters $\mu = 10, k = 0.1, \rho = 0.6, \omega = 0.6,\ t = 0.6$

Table 1
Real drag (T) vs slip parameter (s) at change of micropolarity (e) values at fixed values to frequency parameters $\mu = 10, k = 0.1,\ \rho = 0.6, \omega = 0.6,\ t = 0.6$

T\S	8	16	24	32
5	-2.7986	-3.0061	-3.0561	-3.0786
10	-2.9485	-3.1720	-3.1720	-3.2493
15	-3.0211	-3.2515	-3.2515	-3.3308
20	-3.0639	-3.2982	-3.2982	-3.3786
25	-3.0921	-3.3289	-3.3289	-3.4100
30	-3.1121	-3.3289	-3.3506	-3.4322

Imaginary drag $(T1)$ vs Slip parameter (s) at different micro polarity (e) values are plotted in Figure 4. It was noticed that with a rise in slip (s) values there is an increase in imaginary drag $(T1)$ values and also with a rise in micro polarity (e) values there is a rise in the values of imaginary drag$(T1)$. The numerical results are presented in Table 2.

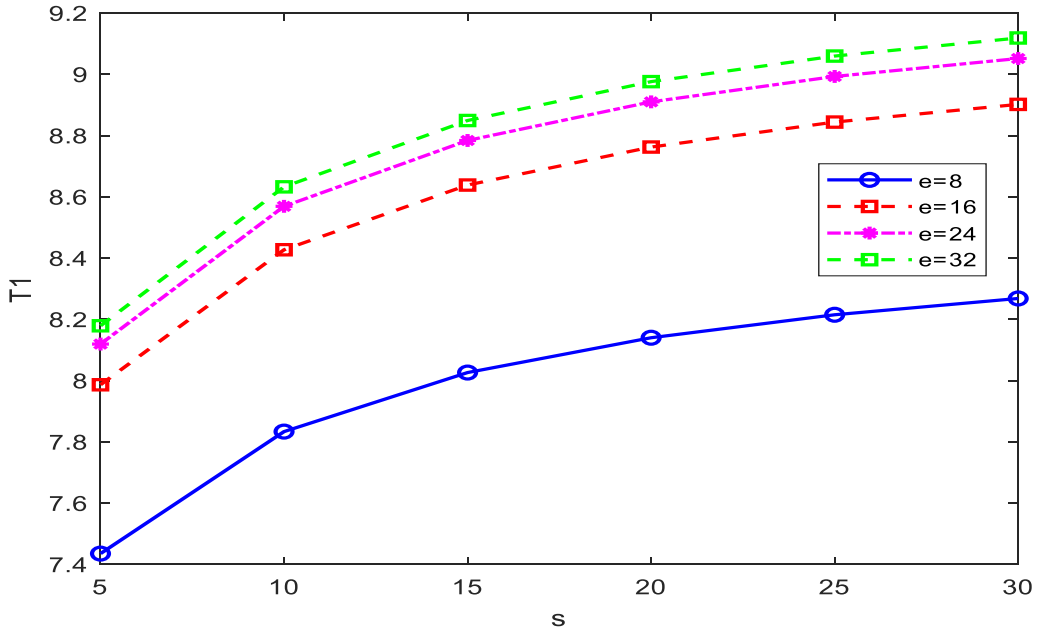

Fig. 4. Imaginary drag $(T1)$ vs slip parameter (s) at change of micropolarity (e) values at fixed values to frequency parameters $\mu = 10, k = 0.1, \rho = 0.6, \omega = 0.6,\ t = 0.6$

Table 2
Imaginary drag $(T1)$ vs slip parameter (s) at change of micropolarity (e) values at fixed values to frequency parameters $\mu = 10, k = 0.1, \rho = 0.6, \omega = 0.6,\ t = 0.6$

S\T	5	10	15	20
5	7.4351	7.9863	8.1192	8.1790
10	7.8334	8.4271	8.5689	8.6325
15	8.0262	8.6384	8.7839	8.8491
20	8.1399	8.7624	8.9100	8.9761
25	8.2149	8.8440	8.9929	9.0595
30	8.2681	8.9017	9.0515	9.1185

Also, for an oscillatory flow of Newtonian liquid beyond a viscous contaminated fluid sphere, the real $(T)$and imaginary part $(T1)$ of drag force variations for slip parameters (s) with varying viscosity

ratio (μ) at fixed values to frequency parameters $k = 0.1, \rho = 0.6, \omega = 0.6,\ t = 0.6$ are presented numerically and are shown in Figure 5 and Figure 6.

Real drag (T) vs Slip parameter (s) at different viscosity ratio (μ) values are plotted in Figure 5. It was noticed that with a rise in slip (s) values there is a fall in real drag (T) and there is fall in the values of real drag $(T)$with a rise in values of viscosity ratio (μ). The numerical results are presented in Table 3.

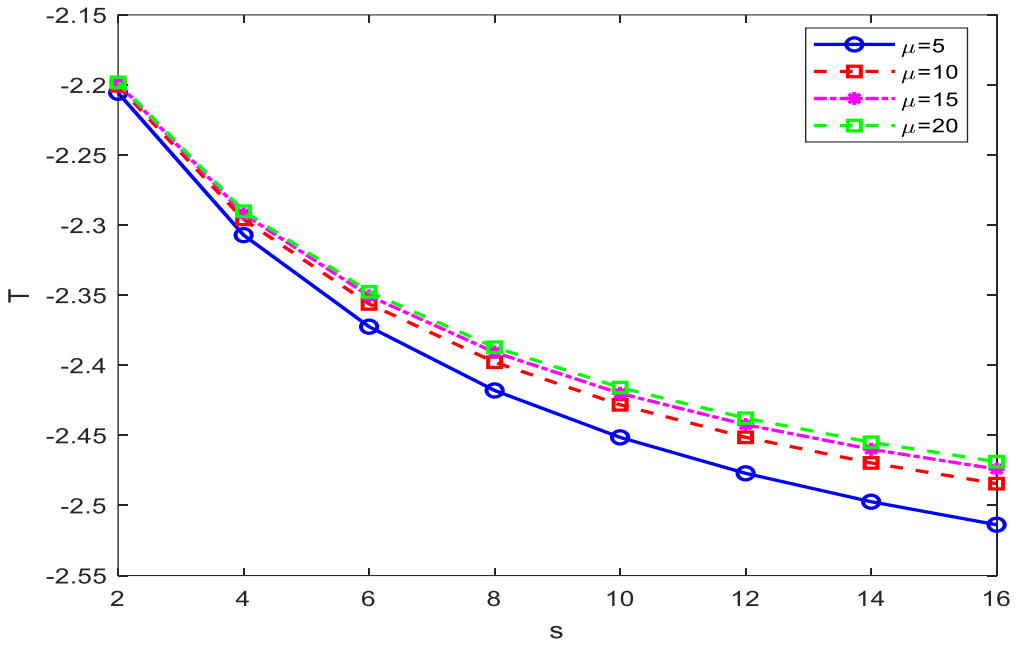

Fig. 5. Real Drag (T) vs slip parameter (s) at Change of viscosity ratio (μ) values at fixed values to frequency parameters $k = 0.1, \rho = 0.6,\ \omega = 0.6, t = 0.6$

Table 3
Real drag(T) vs slip parameter (s) at change of viscosity ratio (μ) values at fixed values to frequency parameters $k = 0.1,\ \rho = 0.6, \omega = 0.6, t = 0.6$

S\T	5	10	15	20
2	-2.2056	-2.2006	-2.1990	-2.1981
4	-2.3071	-2.2959	-2.2920	-2.2900
6	-2.3725	-2.3562	-2.3907	-2.3477
8	-2.4180	-2.3978	-2.4200	-2.3871
10	-2.4514	-2.4282	-2.4200	-2.4159
12	-2.4771	-2.4514	-2.4424	-2.4377
14	-2.4973	-2.4697	-2.4599	-2.4549
16	-2.4844	-2.4844	-2.4741	-2.4688

Imaginary drag $(T1)$ vs Slip parameter (s) at different values of viscosity ratio (μ) are plotted in Figure 6. It was noticed that with a rise in slip (s) values there is a rise in imaginary drag $(T1)$ also and there is fall in the values of imaginary drag $(T1)$with a rise in values of viscosity ratio (μ).The numerical results are presented in Table 4.

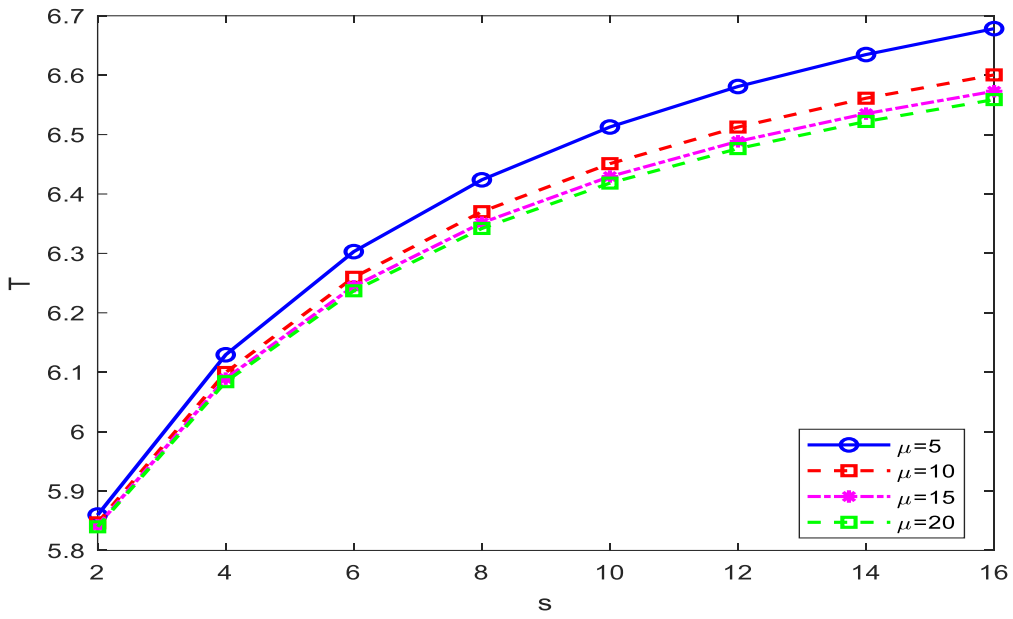

Fig. 6. Imaginary Drag $(T1)$ vs slip parameter (s) at Change of viscosity ratio (μ) values at fixed values to frequency parameters $k = 0.1, \rho = 0.6, \omega = 0.6 \;\; t = 0.6$

Table 4
Imaginary drag$(T1)$ vs slip parameter (s) at change of viscosity ratio (μ) values at fixed values to frequency parameters $k = 0.1, \rho = 0.6, \omega = 0.6, \;\; t = 0.6$

T1/ *S*	**5**	**10**	**15**	**20**
2	5.8596	5.8465	5.8420	5.8398
4	6.1294	6.0995	6.0892	6.0840
6	6.3030	6.2598	6.2447	6.2371
8	6.4239	6.3703	6.3515	6.3420
10	6.5128	6.4511	6.4294	6.4184
12	6.5809	6.5127	6.4887	6.4764
14	6.6347	6.5612	6.5353	6.5221
16	6.6783	6.6005	6.5730	6.5589

4. Conclusions

In this paper, analysis has been done on

i. the oscillatory flow of micropolar beyond a micropolar contaminated fluid sphere and
ii. oscillatory viscous fluid flow beyond a viscous contaminated fluid sphere under the premise of mini amplitude oscillations.

Exact solutions were obtained analytically for the fluid velocity field and microrotation components. The drag force execution on the particle was computed for rectilinear oscillations and few specific cases are reduced. Variations in real drag(T), imaginary drag$(T1)$ w.r.t. micro polarity(e), slip parameter(s) and viscosity ratio (μ) are extracted and graphically displayed and tabulated. It was observed that

i. With a rise in slip parameter(s) values there is a fall in real drag(T) value at varying viscosity ratio (μ) and micro polarity(e) values.

ii. With a rise in slip values there is a rise in imaginary drag$(T1)$ values for different viscosity ratio (μ) and micro polarity(e) values.
iii. For distinct values of slip parameters, with a rise in micro polarity(e) values there is a fall in real drag values(T) and a rise in imaginary drag values$(T1)$.

The scope for extension to intermediate Reynolds numbers using approximate solutions like Homotopy Analysis Method, numerical techniques like Finite Difference Method will pose as interesting problems to researchers. For such studies, this analysis for laminar flow could be beneficial.

Acknowledgement
We sincerely thank to the reviewers for their valuable suggestions in improving this manuscript.

References

[1] Eringen, A. Cemal. "Simple microfluids." *International Journal of Engineering Science* 2, no. 2 (1964): 205-217. https://doi.org/10.1016/0020-7225(64)90005-9
[2] Eringen, A. Cemal. "Linear theory of micropolar elasticity." *Journal of Mathematics and Mechanics* (1966): 909-923. https://doi.org/10.21236/AD0473723
[3] Ariman, T. T. N. D., M. A. Turk, and N. D. Sylvester. "Applications of microcontinuum fluid mechanics." *International Journal of Engineering Science* 12, no. 4 (1974): 273-293. https://doi.org/10.1016/0020-7225(74)90059-7
[4] Lukaszewicz, Grzegorz. *Micropolar fluids: theory and applications*. Springer Science & Business Media, 1999. https://doi.org/10.1007/978-1-4612-0641-5_5
[5] Deo, Satya, and Pankaj Shukla. "Creeping flow of micropolar fluid past a fluid sphere with non-zero spin boundary condition." *International Journal of Engineering and Technology* 1, no. 2 (2012): 67-76. https://doi.org/10.14419/ijet.v1i2.5
[6] Jaiswal, B. R., and B. R. Gupta. "Drag on Reiner-Rivlin liquid sphere placed in a micropolar fluid with non-zero boundary condition for microrotations." *Int. J. of Appl. Math. and Mech* 10, no. 7 (2014): 90-103.
[7] Shukla, Pankaj. "Micropolar fluid past a sphere coated with a thin fluid film." *Indian Journal of Science and Technology* 8, no. 24 (2015): 1-15. https://doi.org/10.17485/ijst/2015/v8i24/80433
[8] Mishra, V., and B. R. Gupta. "Drag experienced by a composite sphere in an axisymmetric creeping flow of micropolar fluid." *Journal of Applied Fluid Mechanics* 11, no. 4 (2018): 995-1004. http://dx.doi.org/10.29252/jafm.11.04.27870. https://doi.org/10.29252/jafm.11.04.27870
[9] Neto, Chiara, Drew R. Evans, Elmar Bonaccurso, Hans-Jürgen Butt, and Vincent SJ Craig. "Boundary slip in Newtonian liquids: a review of experimental studies." *Reports on progress in physics* 68, no. 12 (2005): 2859. https://doi.org/10.1088/0034-4885/68/12/R05
[10] Lok, Y.Y., Pop, I. and Ingham, D.B. "Oblique stagnation slip flow of a micropolar fluid." *Meccanica*, *45*, (2010): 187-198. https://doi.org/10.1007/s11012-009-9236-9
[11] Ashmawy, E. A. "Unsteady Couette flow of a micropolar fluid with slip." *Meccanica* 47, no. 1 (2012): 85-94. https://doi.org/10.1007/s11012-010-9416-7
[12] Gomathy, G., A. Sabarmathi, and Pankaj Shukla. "Creeping flow of non-Newtonian fluid past a fluid sphere with non-zero spin boundary condition", *Advances in Mathematics: Scientific Journal* 9, no. 8 (2020): 5979-5986. https://doi.org/10.37418/amsj.9.8.66
[13] Selvi, R., Pankaj Shukla, and Abhishek Kumar Singh. "Drag on a Reiner-Rivlin liquid sphere embedded in a porous region placed in a micropolar fluid." *Journal of Porous Media* 23, no. 6 (2020): 613-626. https://doi.org/10.1615/JPorMedia.2020027173
[14] Cuenot, B., J. Magnaudet, and B. Spennato. "The effects of slightly soluble surfactants on the flow around a spherical bubble." *Journal of fluid mechanics* 339, (1997): 25-53. https://doi.org/10.1017/S0022112097005053
[15] Dani, Adil, Arnaud Cockx, and Pascal Guiraud. "Direct numerical simulation of mass transfer from spherical bubbles: the effect of interface contamination at low Reynolds numbers." *International Journal of Chemical Reactor Engineering* 4, no. 1 (2006). https://doi.org/10.1017/S0022112097005053
[16] Kishore, Nanda, V. S. Nalajala, and Raj P. Chhabra. "Effects of contamination and shear-thinning fluid viscosity on drag behavior of spherical bubbles." *Industrial & Engineering Chemistry Research* 52, no. 17 (2013): 6049-6056. https://doi.org/10.1021/ie4003188

[17] Sadhal, S. S., and Robert E. Johnson. "Stokes flow past bubbles and drops partially coated with thin films. Part 1. Stagnant cap of surfactant film–exact solution." *Journal of Fluid Mechanics* 126 (1983): 237-250. https://doi.org/10.1017/S0022112083000130
[18] Nalajala, Venkata Swamy, and Nanda Kishore. "Drag of contaminated bubbles in power-law fluids." *Colloids and Surfaces A: Physicochemical and Engineering Aspects* 443 (2014): 240-248. https://doi.org/10.1016/j.colsurfa.2013.11.014
[19] Murthy, JV Ramana, and M. Phani Kumar. "Exact solution for flow over a contaminated fluid sphere for Stokes flow." In *Journal of Physics: Conference Series*, vol. 662, no. 1, p. 012016. IOP Publishing, 2015. https://doi.org/10.1088/1742-6596/662/1/012016
[20] Saboni, Abdellah, Silvia Alexandrova, and M. Kaarsheva. "Effects of interface contamination on mass transfer into a spherical bubble." *Journal of Chemical Technology and Metallurgy* 50, no. 5 (2015): 589-596.
[21] Hocquart, R., and E. J. Hinch. "The long-time tail of the angular-velocity autocorrelation function for a rigid Brownian particle of arbitrary centrally symmetric shape." *Journal of Fluid Mechanics* 137 (1983): 217-220. https://doi.org/10.1017/S0022112083002360
[22] Hurd, Alan J., Noel A. Clark, Richard C. Mockler, and William J. O'Sullivan. "Friction factors for a lattice of Brownian particles." *Journal of fluid mechanics* 153 (1985): 401-416. https://doi.org/10.1017/S0022112085001318
[23] Rao, SK Lakshmana, and P. Bhujanga Rao. "The oscillations of a sphere in a micropolar fluid." *International Journal of Engineering Science* 9, no. 7 (1971): 651-672. https://doi.org/10.1016/0020-7225(71)90068-1
[24] Charya, D. Srinivasa, and T. K. V. Iyengar. "Drag on an axisymmetric body performing rectilinear oscillations in a micropolar fluid." *International journal of engineering science* 35, no. 10-11 (1997): 987-1001. https://doi.org/10.1016/S0020-7225(97)00103-1
[25] Naveed, Muhammad, Muhammad Imran, and Zaheer Abbas. "Curvilinear flow of micropolar fluid with Cattaneo–Christov heat flux model due to oscillation of curved stretchable sheet." *Zeitschrift für Naturforschung A* 76, no. 9 (2021): 799-821. https://doi.org/10.1515/zna-2021-0006
[26] Ilyas, Rushdan Ahmad, Salit Mohd Sapuan, Mohamad Ridzwan Ishak, and Edi Syams Zainudin. "Water transport properties of bio-nanocomposites reinforced by sugar palm (Arenga Pinnata) nanofibrillated cellulose." *Journal of Advanced Research in Fluid Mechanics and Thermal Sciences* 51, no. 2 (2018): 234-246.
[27] Mishra, S. R., I. Khan, Q. M. Al-Mdallal, and T. Asifa. "Free convective micropolar fluid flow and heat transfer over a shrinking sheet with heat source." *Case studies in thermal engineering* 11 (2018): 113-119. https://doi.org/10.1016/j.csite.2018.01.005
[28] Ali, Bagh, Anum Shafiq, Imran Siddique, Qasem Al-Mdallal, and Fahd Jarad. "Significance of suction/injection, gravity modulation, thermal radiation, and magnetohydrodynamic on dynamics of micropolar fluid subject to an inclined sheet via finite element approach." *Case Studies in Thermal Engineering* 28 (2021): 101537. https://doi.org/10.1016/j.csite.2021.101537
[29] Siddiqa, Sadia, Naheed Begum, Md Anwar Hossain, Muhammad Nasir Abrar, Rama Subba Reddy Gorla, and Qasem Al-Mdallal. "Effect of thermal radiation on conjugate natural convection flow of a micropolar fluid along a vertical surface." *Computers & Mathematics with Applications* 83 (2021): 74-83. https://doi.org/10.1016/j.camwa.2020.01.011
[30] Jamali, Muhammad Sabaruddin Ahmad, Zuhaila Ismail, and Norsarahaida Saidina Amin. "Effect of Different Types of Stenosis on Generalized Power Law Model of Blood Flow in a Bifurcated Artery." *Journal of Advanced Research in Fluid Mechanics and Thermal Sciences* 87, no. 3 (2021): 172-183. https://doi.org/10.37934/arfmts.87.3.172183
[31] Al-Dailami, Anas, Iwamoto Koji, Imran Ahmad, and Masafumi Goto. "Potential of Photobioreactors (PBRs) in Cultivation of Microalgae." *Journal of Advanced Research in Applied Sciences and Engineering Technology* 27, no. 1 (2022): 32-44. https://doi.org/10.37934/araset.27.1.3244
[32] Kumar Manoj, and Aadil Hashim Saifi. "Marangoni Convection in Liquid Bridges due to a Heater/Cooler Ring." *Journal of Advanced Research in Numerical Heat Transfer* 12, no. 1 (2023): 18-25.